Nanoparticles

DOI: 10.1002/ange.201311254

In Situ Total X-Ray Scattering Study of WO_3 Nanoparticle Formation under Hydrothermal Conditions**

*Dipankar Saha, Kirsten M. Ø. Jensen, Christoffer Tyrsted, Espen D. Bøjesen, Aref Hasen Mamakhel, Ann-Christin Dippel, Mogens Christensen, and Bo B. Iversen**

Abstract: *Pair distribution function analysis of in situ total scattering data recorded during formation of WO_3 nanocrystals under hydrothermal conditions reveal that a complex precursor structure exists in solution. The WO_6 polyhedra of the precursor cluster undergo reorientation before forming the nanocrystal. This reorientation is the critical element in the formation of different hexagonal polymporphs of WO_3.*

Presently, only little is known about how precursor solutions under solvothermal conditions react to form solid precipitates, which eventually transform into nanocrystals. In situ total scattering studies in combination with pair distribution function (PDF) analysis allows unique insight into the mechanisms governing the nanocrystal formation as it can extract precise atomic scale structural information from solutions, amorphous solids, nanosized structures, and also from crystals.[1] Applications of in situ total scattering methods are gaining tremendous attention,[2] but there are very few examples where these methods have been applied to study reaction mechanisms of nanoparticle formation under elevated temperature and pressure conditions.[3] The highly complex formation mechanisms can be monitored by using a unique experimental setup,[4] which enables direct probing of the reaction mixture with high-energy synchrotron X-rays in real time. Herein we show how time-resolved in situ total scattering can reveal hitherto unknown structural information about the initial transformation of molecular precursor complexes into crystalline nanoparticles.

Tungsten trioxide (WO_3) has been widely investigated as an electrochromic material to manipulate solar radiation, which is very important for deriving sustainable energy[5] or for applications in smart windows.[6] WO_3 exists in a series of stable solid phases at different temperatures from the α phase to the ε phase, as well as a metastable hexagonal phase. These solids have been used for dye-sensitized solar cells, smart windows, and gas sensors owing to their excellent electrochemical, electrochromic, photochromic, and gas sensing properties,[7] and also metastable solids are of great importance owing to their properties.[8] The desirable properties depend on inherent structural, morphological, and compositional characteristics as well as the specific synthesis procedures. Recently ultraviolet photoresponse properties have been demonstrated in nanostructured WO_3.[9] Nanostructuring of these compounds therefore plays a crucial role in manipulating the properties, and this makes it essential to study the complex reaction mechanisms leading to the formation of nanocrystals.

In the present study, an aqueous precursor solution of ammonium metatungstate $(NH_4)_6H_2W_{12}O_{40}{\cdot}x\,H_2O$ was heated under high-pressure conditions using a specially designed in situ reactor.[4] Figure 1 shows the evolution of

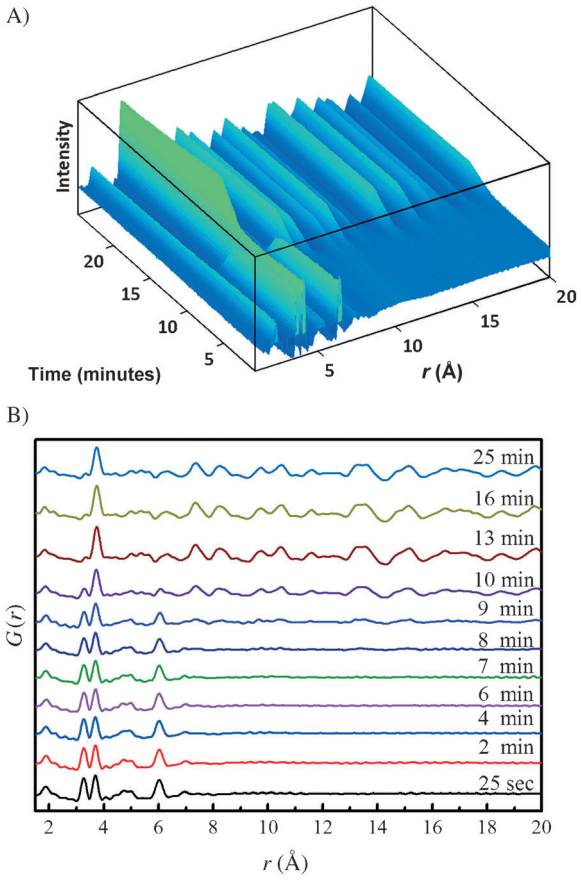

Figure 1. A) Evolution of the PDF with respect to time at 250 °C. B) Selected PDFs illustrating the reaction progress at 250 °C.

[*] Dr. D. Saha, Dr. K. M. Ø. Jensen, Dr. C. Tyrsted, E. D. Bøjesen, Dr. A. H. Mamakhel, Dr. M. Christensen, Prof. Dr. B. B. Iversen
Center for Materials Crystallography
Department of Chemistry and iNANO, Aarhus University
Langelandsgade 140, 8000 Aarhus (Denmark)
E-mail: bo@chem.au.dk
Dr. A.-C. Dippel
Deutsches Elektronen-Synchrotron DESY
Photon Science, Notkestrasse 85, 22607 Hamburg (Germany)

[**] This work was supported by the Danish National Research Foundation (DNRF93) and the Danish Research Council for Nature and Universe (Danscatt). We thank DESY in Germany and MAX-lab in Sweden for synchrotron beamtime.

Supporting information for this article is available on the WWW under http://dx.doi.org/10.1002/anie.201311254.

the PDF with respect to time at 250 °C obtained for the dissolved precursor solution. The precursor structure in solution remains similar before and immediately after the heating is initiated, as there was no change in scattering observed after the heater was switched on. A representative data set obtained 25 s after initiation of heating was subjected to structural modeling analysis, and it revealed that WO_6 octahedra form a cluster by corner- and edge-sharing (Figure 2B). The first two peaks at 1.87 Å and 2.22 Å correspond to W–O bond distances, which agree well with the previously reported values.[10] The shortest W–W distances (3.28 Å) arise from edge sharing of WO_6 octahedra, whereas the W–W distances of 3.68 Å arise from corner sharing of WO_6 octahedra. The presence of a noticeable peak at 6.02 Å is due to the second coordination sphere of W–W distances and it substantiates the formation of the cluster. The fitted model for the structure of the precursor complex is shown in Figure 2B. It is of interest to note that the absence of any correlations in the PDF beyond a distance of about 7 Å indicates the presence of local ordering only. A similar structure has been observed in the crystal structure of $(NH_4)_{10}(H_2W_{12}O_{42})\cdot(H_2O)_4$,[11] but no information has previously been available on the structural characteristics of the molecular species in solution. As the reaction progresses there is no significant change observed in the PDF until after 7 min of heating. Here the peak intensities at 3.28 Å and 6.02 Å decrease (Figure 1B), indicating that the edge-sharing octahedra are being converted into corner-sharing octahedra. It is noteworthy that while the octahedra locally become reoriented there is no evidence of long range order. After 10 min. of heating, the nuclei in the solution abruptly cluster together and form crystalline particles. The whole process of formation of nanoparticles from precursor nuclei occurs within about 3 min. Data were also collected at 270 °C and 300 °C to see the effect of reaction temperature on the reaction rate, and at higher temperatures the initiation of nanoparticle formation becomes faster. In the case of 270 °C and 300 °C reaction temperatures, the time elapsed before nanoparticle formation were about 8 and about 5 min, respectively (see the Supporting Information), but the overall mechanism remains unchanged. Therefore, it is suggested that the molecular complex in the precursor solution undergoes a reorientation of the octahedral building blocks prior to the formation of nanoparticles. The time required for the nuclei to arrange themselves depends on the synthesis temperature. Once the necessary activation energy is gained by all the nuclei, they aggregate to form larger-sized nanoparticles. These observations are substantiated by the in situ PXRD measurements discussed below. Formation mechanisms for WO_3 nanoparticles from aqueous and non-aqueous solution have recently been reported,[12] but no information was provided on precursor structure.

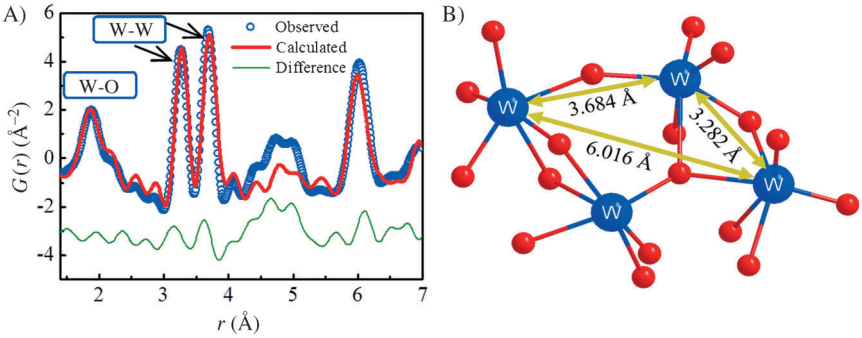

Figure 2. A) PDF for the precursor solution. B) Molecular cluster present in the precursor solution.

Rietveld refinement was carried out on in situ PXRD data collected for the same experimental conditions as the in situ total scattering measurements ($T = 250$, 270, 300 °C; $P = 250$ bar). The PXRD data of WO_3 can be indexed in a hexagonal crystal system with space group *P6/mmm* using the H1 crystal structure of WO_3.[13] This structure consists of corner sharing WO_6 octahedra, and the Rietveld refinements improve when the crystallites are allowed to elongate along the *c*-axis; that is, the nanocrystals are rod-shaped (see the Supporting Information). At 250 °C, a sudden formation of 10 nm nanocrystals is observed after about 11 min of reaction. Similar abrupt formation of nanocrystals is also observed at the two other temperatures, and as the reaction temperature increases, the nucleation time becomes shorter, in accordance with the in situ PDF analysis.

Further PDF analysis was carried out on the in situ total scattering data set obtained after 25 min of reaction at 250 °C using the H1 structural model. This model provides a good description of the long range order (5.5–20 Å) in the crystal structure (see the Supporting Information), but the H1 structure cannot explain the local structure, such as the shoulder peak at 2.22 Å (Figure 3). However, two kinds of *h*-WO_3 structures have been reported,[10,13] and the space group of the other *h*-WO_3 polymorph called H2 is $P6_3/mcm$. The H2 structural model was fitted to the local structure only, and indeed the H2 model accounts for the shoulder peak at 2.22 Å (Figure 3). The H2 model contains half occupied disordered oxygen positions, resulting in the longer W–O bond distance at 2.22 Å. Figure 3B illustrates the difference in local structure between the H1 and H2 models.

The question arises as to whether the in situ information is transferable to the synthesis conditions used in a chemical laboratory. To explore this aspect, WO_3 was synthesized using the same precursor in a supercritical flow reactor.[14] Interestingly the WO_3 synthesis product obtained from the capillary reactor crystallizes with the H1 crystal structure, whereas the flow synthesis yields the H2 structure (see the Supporting Information for detailed Rietveld refinement). The in situ PDF analysis revealed that before crystal formation the precursor complex undergoes a reorientation of WO_6 octahedra from edge-sharing to corner-sharing. In the flow reactor, the reaction time is very short, and therefore it may be suggested that in case of flow synthesis the octahedra in the

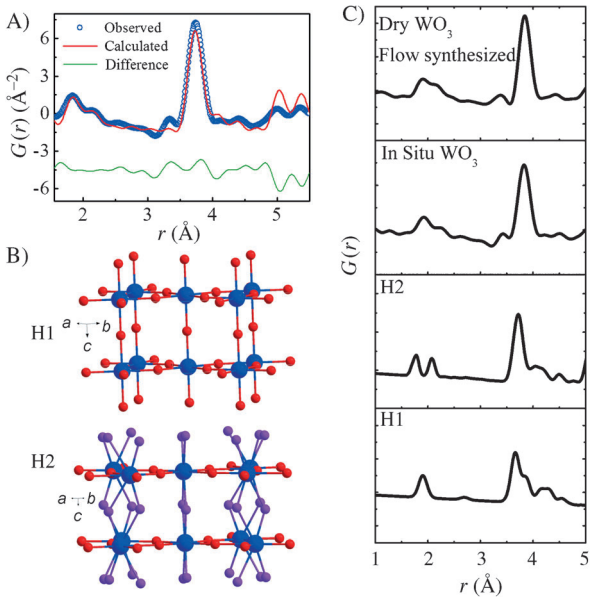

Figure 3. A) PDF fitted with the H2 model for local structure only. B) The H1 and H2 structures crystal structures. C) Simulated PDF from the H1 and H2 structures in comparison with in situ and supercritical flow synthesized WO_3.

precursor complex do not have adequate time to reorient themselves into the ordered H1 structure, and this results in half-occupied disordered oxygen positions (H2 structure). In other words, the disordered oxygen is reminiscent of the edge-sharing octahedra in the precursor complex. The very fast heating rate of the in situ reactor provides a reaction environment mimicking the flow conditions rather than the much slower reaction conditions present in a classical batch reactor. The in situ PXRD data obtained after 20 min correspond to the H1 structure (thus mimicking the batch synthesis), and the data measured closer and closer to the initiation of crystallization (that is, ca. 11 min. at 250 °C) do not have sufficient peak resolution to reveal the subtle differences in the diffraction patterns of the H1 and H2 structures. The reorientation of the octahedra from edge sharing (H2) to corner sharing (H1) occurs in the first few minutes after crystallization.

In conclusion, in situ X-ray scattering studies of solvothermal reactions provide a unique opportunity to investigate previously unexplored reaction mechanisms for the formation of solids from solution. The present study on WO_3 establishes the complex precursor structure and the reaction pathways, and it also rationalizes the formation of two different hexagonal phases of WO_3.

Experimental Section

An aqueous solution (0.2 M) of ammonium metatungstate $(NH_4)_6H_2W_{12}O_{40}\cdot xH_2O$ (Sigma Aldrich, >99 %) was used for the in situ syntheses in a custom-made capillary reactor pressurized to 250 bar and heated to temperatures of 250, 270, and 300 °C. The in situ total scattering PDF experiments were carried out at beamline P02.1 at PETRA III, DESY, Germany. In situ PXRD experiments were performed at beamline I711 at MAX-lab in Sweden. The X-ray wavelengths for the in situ PDF and PXRD experiments were 0.207 and 1.000 Å, respectively. The experimental setup used for both the in situ total scattering and PXRD measurements has been described in detail by Becker et al.[4] The integrated total scattering data were analyzed with the PDFgetX3 program.[15] Prior to the Fourier transformation, the data were corrected for background scattering using measurements in deionized water in the same capillary at the appropriate temperatures. The resulting PDFs were refined using PDFgui.[16] The PXRD data were integrated using Fit2D,[17] and Rietveld refinement was carried out using the FullProf Suite.[18] Flow synthesis was carried out in a supercritical flow reactor described in detail elsewhere.[19] The reactor temperature was kept at 350 °C with a pressure of 250 bar. Water was used in the solvent string and ammonium metatungstate was used in the precursor string. The mixing was carried out in T-piece geometry.

Received: December 28, 2013
Published online: February 26, 2014

Keywords: hydrothermal synthesis · nanoparticles · pair distribution functions · powder X-ray diffraction · tungsten

[1] S. J. L. Billinge, M. G. Kanatzidis, *Chem. Commun.* **2004**, 749–760.
[2] a) S. M. Oxford, P. L. Lee, P. J. Chupas, K. W. Chapman, M. C. Kung, H. H. Kung, *J. Phys. Chem. C* **2010**, *114*, 17085–17091; b) F. Zhang, P. J. Chupas, S. L. A. Lui, J. C. Hanson, W. A. Caliebe, P. L. Lee, S.-W. Chan, *Chem. Mater.* **2007**, *19*, 3118–3126; c) P. J. Chupas, S. Chaudhuri, J. C. Hanson, X. Qiu, P. L. Lee, S. D. Shastri, S. J. L. Billinge, C. P. Grey, *J. Am. Chem. Soc.* **2004**, *126*, 4756–4757; d) K. W. Chapman, P. J. Chupas, C. J. Kepert, *J. Am. Chem. Soc.* **2005**, *127*, 11232–11233; e) M. A. Newton, K. W. Chapman, D. Thompsett, P. J. Chupas, *J. Am. Chem. Soc.* **2012**, *134*, 5036–5039.
[3] a) K. M. Ø. Jensen, M. Christensen, P. Juhas, C. Tyrsted, E. D. Bøjesen, N. Lock, S. J. L. Billinge, B. B. Iversen, *J. Am. Chem. Soc.* **2012**, *134*, 6785–6792; b) C. Tyrsted, K. M. Ø. Jensen, E. D. Bøjesen, N. Lock, M. Christensen, S. J. L. Billinge, B. B. Iversen, *Angew. Chem.* **2012**, *124*, 9164–9167; *Angew. Chem. Int. Ed.* **2012**, *51*, 9030–9033.
[4] J. Becker, M. Bremholm, C. Tyrsted, B. Pauw, K. M. O. Jensen, J. Eltzholt, M. Christensen, B. B. Iversen, *J. Appl. Crystallogr.* **2010**, *43*, 729–736.
[5] a) C. G. Granqvist, *Nat. Mater.* **2006**, *5*, 89–90; b) E. Avendaño, L. Berggren, G. A. Niklasson, C. G. Granqvist, A. Azens, *Thin Solid Films* **2006**, *496*, 30–36; c) C. Guo, S. Yin, T. Sato, *Rev. Adv. Sci. Eng.* **2012**, *1*, 235–263.
[6] C. G. Granqvist, *Sol. Energy Mater. Sol. Cells* **2012**, *99*, 1–13.
[7] a) H. Zheng, Y. Tachibana, K. Kalantar-zadeh, *Langmuir* **2010**, *26*, 19148–19152; b) G. A. Niklasson, C. G. Granqvist, *J. Mater. Chem.* **2007**, *17*, 127–156; c) D. T. Gillaspie, R. C. Tenent, A. C. Dillon, *J. Mater. Chem.* **2010**, *20*, 9585–9592; d) Y. Takeda, N. Kato, T. Fukano, A. Takeichi, T. Motohiro, S. Kawai, *J. Appl. Phys.* **2004**, *96*, 2417–2422; e) M. Shibuya, M. Miyauchi, *Adv. Mater.* **2009**, *21*, 1373–1376; f) L. F. Zhu, J. C. She, J. Y. Luo, S. Z. Deng, J. Chen, N. S. Xu, *J. Phys. Chem. C* **2010**, *114*, 15504–15509.
[8] C. Feldmann, *Angew. Chem.* **2013**, *125*, 7762–7763; *Angew. Chem. Int. Ed.* **2013**, *52*, 7610–7611.
[9] N. Huo, S. Yang, Z. Wei, J. Li, *J. Mater. Chem. C* **2013**, *1*, 3999–4007.
[10] J. Oi, A. Kishimoto, T. Kudo, M. Hiratani, *J. Solid State Chem.* **1992**, *96*, 13–19.

[11] H. Evans Jr., in *Polyoxometalates*: *From Platonic Solids to Anti-Retroviral Activity*, *Vol. 10* (Eds.: M. Pope, A. Müller), Springer, Dordrecht, **1994**, pp. 71 – 86.
[12] a) I. Olliges-Stadler, M. D. Rossell, M. J. Suess, B. Ludi, O. Bunk, J. S. Pedersen, H. Birkedal, M. Niederberger, *Nanoscale* **2013**, *5*, 8517 – 8525; b) R. Kiebach, N. Pienack, W. Bensch, J.-D. Grunwaldt, A. Michailovski, A. Baiker, T. Fox, Y. Zhou, G. R. Patzke, *Chem. Mater.* **2008**, *20*, 3022 – 3033; c) Y. Zhou, N. Pienack, W. Bensch, G. R. Patzke, *Small* **2009**, *5*, 1978 – 1983.
[13] B. Gerand, G. Nowogrocki, J. Guenot, M. Figlarz, *J. Solid State Chem.* **1979**, *29*, 429 – 434.
[14] P. Hald, J. Becker, M. Bremholm, J. S. Pedersen, J. Chevallier, S. B. Iversen, B. B. Iversen, *J. Solid State Chem.* **2006**, *179*, 2674 – 2680.
[15] P. Juhás, T. Davis, C. L. Farrow, S. J. L. Billinge, *J. Appl. Crystallogr.* **2013**, *46*, 560 – 566.
[16] C. L. Farrow, P. Juhas, J. W. Liu, D. Bryndin, E. S. Božin, J. Bloch, T. Proffen, S. J. L. Billinge, *J. Phys. Condens. Matter* **2007**, *19*, 335219 – 335226.
[17] A. Hammersley, S. Svensson, M. Hanfland, A. Fitch, D. Hausermann, *High Pressure Res.* **1996**, *14*, 235 – 248.
[18] J. Rodríguez-Carvajal, *Phys. B* **1993**, *192*, 55 – 69.
[19] N. Lock, M. Christensen, K. M. Ø. Jensen, B. B. Iversen, *Angew. Chem.* **2011**, *123*, 7183 – 7185; *Angew. Chem. Int. Ed.* **2011**, *50*, 7045 – 7047.

